shown in Fig. 11 are interesting. Their formation should be enhanced by suitable doping, for example with Ba^{2+} or similar disposable ions, in addition to the Ga, Mg or Al ions required to produce {210} defect-pairs. A systematic study of the preparative conditions is required. The intersection structures may act as nuclei for phase transformations or transitions. The former has been observed for the low- to high-temperature transformation in the Fe–Ti–O and Cr–Ti–O systems (Bursill, Netherway & Grey, 1978), where the intersections aggregate and order producing a high-temperature structure having minimum elastic strain energy.

The observation that some defect-pairs terminate just short of possible intersections (Fig. 7) suggests that some of the intersections require higher thermodynamic driving force. A study of the mobility of such structures (experimentally using a high-temperature goniometer and theoretically, in terms of atomic-diffusion mechanisms and energies of formation, interaction and migration) should prove interesting. However, even at this stage, it should be appreciated that such energy terms will largely determine the kinetics of the reaction between rutile and its dopants. Similar intersection structures have been observed in TiO_x (Bursill, Hyde, Terasaki & Watanabe, 1969); here there are numerous possibilities, with eight {132} and four {101} contributing. These must make significant contributions to the very large hysteresis between reduction and oxidation paths found by thermodynamic studies (Merritt & Hyde, 1973).

This work was financially supported by the Australian Research Grants committee and the University of Melbourne. The author thanks Mr G. G. Stone for preparing the ion-thinned specimen.

References

BURSILL, L. A. (1979*a*). *Acta Cryst.* B**35**, 530–538.

BURSILL, L. A. (1979*b*). *Acta Cryst.* Submitted.

BURSILL, L. A. & BARRY, J. C. (1977). *Philos. Mag.* **36**, 497–510.

BURSILL, L. A., HYDE, B. G., TERASAKI, O. & WATANABE, D. (1969). *Philos. Mag.* **20**, 347–359.

BURSILL, L. A. & NETHERWAY, D. J. (1979). *Acta Cryst.* Submitted.

BURSILL, L. A., NETHERWAY, D. J. & GREY, I. E. (1978). *Nature (London)*, **272**, 405–410.

BURSILL, L. A. & STONE, G. G. (1975). *Philos. Mag.* **32**, 1151–1158.

BURSILL, L. A. & STONE, G. G. (1979*a*). *Acta Cryst.* Submitted.

BURSILL, L. A. & STONE, G. G. (1979*b*). *Philos. Mag.* Submitted.

BURSILL, L. A. & WILSON, A. R. (1977). *Acta Cryst.* A**33**, 672–676.

GIBB, R. M. & ANDERSON, J. S. (1972). *J. Solid State Chem.* **5**, 212–225.

LLOYD, D. J., GREY, I. E. & BURSILL, L. A. (1976). *Acta Cryst.* B**32**, 1756–1761.

MERRITT, R. R. & HYDE, B. G. (1973). *Philos. Trans. R. Soc. London. Ser. A*, **274**, 627–661.

STONE, G. G. & BURSILL, L. A. (1977). *Philos. Mag.* **35**, 1397–1412.

Acta Cryst. (1979). A**35**, 458–462

X–N and *X–X* ($1s^2$ Core) Maps for Cyanuric Acid

BY A. KUTOGLU AND C. SCHERINGER

Institut für Mineralogie der Universität Marburg, D 3550 *Marburg, Federal Republic of Germany*

(*Received* 4 *December* 1978; *accepted* 18 *January* 1979)

Abstract

X–N maps and *X–X* ($1s^2$ core parameter) maps of cyanuric acid, $C_3H_3N_3O_3$, at 100 K are presented. The differences in scale and in the atomic parameters have large effects ($\leq 0{\cdot}4$ e Å^{-3}) on the difference density at the nuclei but smaller effects ($\leq 0{\cdot}15$ e Å^{-3}) on the bond density distributions. In particular, the density distribution around the O atoms, where polarization is likely to occur, is different in the two types of maps. It is concluded that, in these regions, the *X–N* maps yield the more reliable results.

0567-7394/79/030458-05$01.00

Introduction

From a previously refined model of the electron density distribution in cyanuric acid (100 K X-ray data of Verschoor & Keulen, 1971), the positional and thermal parameters of the $1s^2$ atomic cores were determined (Kutoglu & Hellner, 1978). *X–X* ($1s^2$) and *X–N* maps were calculated with the neutron parameters of Coppens & Vos (1971). Owing to an error in the data transmission of the form-factor curve of the O atom, both maps were falsified. The corrected maps are given in this paper (Figs. 1 and 2).

The X–N and X–$X(1s^2)$ maps differ from each other in some respects, and one would like to know how these deviations should be interpreted. The deviations are probably caused by the differences in the two sets of parameters and by the differences in scale. With the neutron parameters, a problem arises in that these parameters were determined by Coppens & Vos (1971) for a temperature of about 125 K, whereas the X-ray data were collected by Verschoor & Keulen (1971) at about 95 K. The nuclear thermal parameters were calculated for the temperature of the X-ray data by

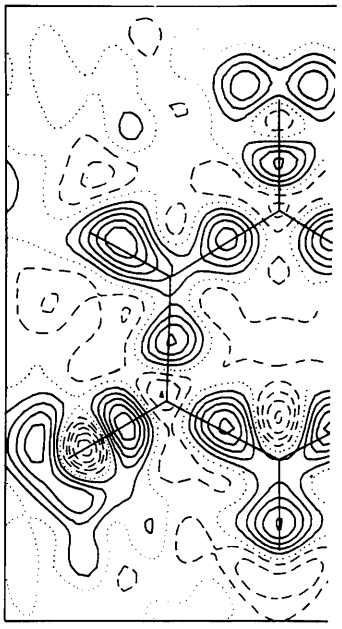

(*a*)

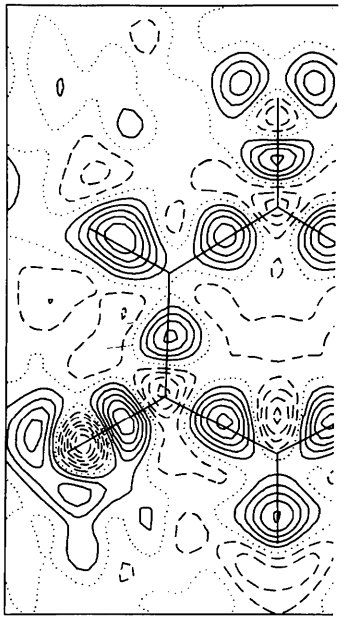

(*b*)

Fig. 1. X–N maps of cyanuric acid at 100 K in the plane of the molecule. Contour interval 0·1 e Å^{-3}; positive contours, full lines; zero, dotted lines; negative, dashed lines. (*a*) Scale factor = 1·0 from refinement of free-atom model. (*b*) Scale factor = 1·0062 from refinement of molecular-density model with neutron atomic parameters.

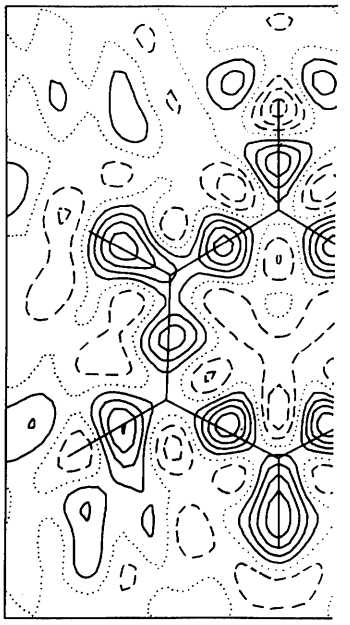

(*a*)

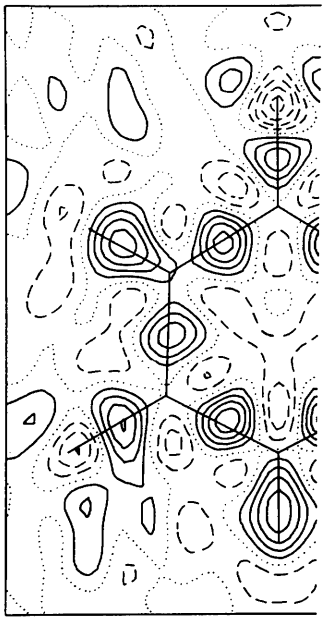

(*b*)

Fig. 2. X–$X(1s^2$-core parameter) maps. (*a*) Scale factor = 1·0139 from refinement of free-atom model. (*b*) Scale factor = 1·0181 from refinement of molecular-density model. Contours as in Fig. 1.

reducing the 125 K nuclear thermal parameters by a constant factor of 0·728 (Coppens & Vos, 1971). Such a constant reduction of all the thermal parameters in this temperature range cannot safely be assumed. On the other hand, the determination of the atomic and density parameters from the X-ray data presents difficulties, since high correlations between the $1s^2$ parameters and the density parameters of the model occur. Thus, the $1s^2$ positional and thermal parameters were determined by Kutoglu & Hellner (1978) only at the end of the refinement of the density model, and by alternately excluding sets of highly correlated parameters from the refinement.

In this paper we shall discuss the differences between the X–N and X–$X(1s^2)$ maps as being caused by the differences between the two sets of parameters. In order to decide whether or not there are systematic differences, we compare the two sets of parameters by statistical tests (half-normal probability plots and χ^2 tests). Ultimately, we try to find out which of the two types of maps is more likely to be valid.

Comparison of parameter sets, and statistical tests

The positions of the C, N, and O atoms agree within 0·001 Å, except for O(2) and C(2). The $1s^2$ position of O(2) is displaced by 0·004 Å relative to the neutron position in such a way as to lengthen the C—O bond, and the $1s^2$ position of C(2) is displaced by 0·002 Å in the y direction, see Kutoglu & Hellner (1978, Fig. 2). Coppens (1971) also determined the positional parameters of the atomic cores of the C, N, O atoms in his double atom refinement. He found agreement between X-ray and neutron parameters for the C and N atoms, but a deviation of 0·006 Å for O(2), and of 0·003 Å for O(1). The thermal $1s^2$ parameters are usually a little larger than the neutron parameters, except for O(1). Hence, the $1s^2$ scale factors (as factors of F_c) are larger than the scale factors obtained with the neutron parameters, and thus partially compensate for the trend in the thermal parameters [not, however, for O(1)].

The half-normal probability plots (Abrahams & Keve, 1971) are given in Figs. 3(*a*) (positional parameters) and 3(*b*) (thermal parameters). Departure from linearity is more pronounced for the positional parameters, but does not appear to be large for the thermal parameters (H atom parameters are excluded). The outermost points in the plots, where the difference between two corresponding parameters is largest relative to the e.s.d.'s, refer to the pairs of y(C2), y,z(O2) in Fig. 3(*a*), and to the pairs of U_{33}, U_{11}(N1), U_{33}(C2), U_{11}(N2) in Fig. 3(*b*). For the positional parameters, systematic differences between the neutron and $1s^2$ parameters probably cannot be excluded, whereas for the thermal parameters, we may classify

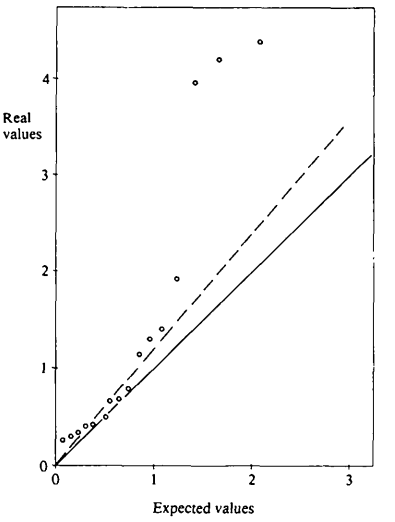

(*a*)

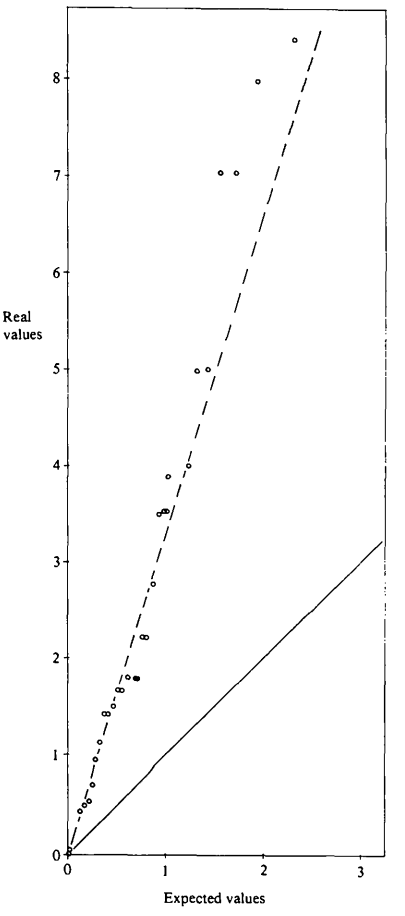

(*b*)

Fig. 3. Half-normal probability plots for the observed differences between neutron diffraction parameters and $1s^2$-core parameters for cyanuric acid at 100 K. Unit slope, full line; estimated slopes, dashed lines. (*a*) Positional parameters. (*b*) Thermal parameters (without hydrogen parameters).

the observed weighted differences between the two sets as nearly random.

The slopes in Fig. 3 are about 1·2 and 3·25, which means that the e.s.d.'s of the positional and thermal parameters, as obtained from the refinement, are underestimated by factors of about 1/1·2 and 1/3·25 respectively. The large underestimate for the e.s.d.'s of the thermal parameters is not unreasonable, since a good fit of these parameters to the data is often obtained by the absorption of many types of error into the thermal parameters. This situation usually escapes detection but a half-normal plot reveals it. In order to perform the χ^2 test, we have to rescale the given e.s.d.'s to their (approximate) true values by the slopes of the plots, otherwise we may draw erroneous conclusions from the test.

We calculated the χ^2 test (Hamilton, 1969) both for all 16 pairs of positional parameters and for only 13 pairs, since the half-normal plot indicates that three points (three pairs of parameters) deviate from a supposed straight line. For the first 13 positional parameters of the plot, we obtain the unscaled experimental value of $\chi^2_{\text{exp}} = 11{\cdot}1$ and the correspondingly scaled value $11{\cdot}1/1{\cdot}2^2 = 7{\cdot}7$. The theoretical value $\chi^2_{13,0{\cdot}5} = 12{\cdot}3$ suggests that no significant differences between the two sets of the 13 positional parameters exist. If we include the three pairs of parameters corresponding to the outermost points in Fig. 1(*a*), we find for the scaled experimental value $\chi^2_{\text{exp}} = 44{\cdot}3$ and $\chi^2_{16,0{\cdot}001} = 39{\cdot}3$. This shows that the (weighted) deviations between the y(C2), y,z(O2) parameters cannot be interpreted as being drawn from a normal distribution, and thus are due to some type of systematic error.

For the first 23 pairs of parameters of Fig. 3(*b*) we find $\chi^2_{\text{exp, scaled}} = 8{\cdot}6$; $\chi^2_{23,0{\cdot}5} = 22{\cdot}3$, and for all 30 parameters $\chi^2_{\text{exp, scaled}} = 36{\cdot}9$; $\chi^2_{30,0{\cdot}1} = 40{\cdot}3$. Thus, for the thermal parameters, we cannot reject the hypothesis that the weighted deviations between the two sets of parameters are drawn from a normal distribution; for the first 23 parameters even on the 0·5 level of significance.

X–N and *X–X*(1*s*²) maps

The form-factor curves for all (neutral) atoms were taken from *International Tables for X-ray Crystallography* (1974). The 942 X-ray data were used which remain when the 25 data with $\sigma(F) = 100$ are excluded from Verschoor & Keulen's (1971) total data set. With the scale factor of 1·0, as obtained from the refinement with the free-atom model, our *X–N* map of Fig. 1(*a*) should be equal to that of Coppens & Vos (1971) (CV map); however, there are some intolerable deviations. In order to check our map, we calculated it with two independent programs. The most important deviations are the following: in the CV map, there is an additional outer lone-pair peak (0·2 e Å^{-3}) at O(1) where we have a zero contour; the lone pairs at O(2) form a single (unresolved) peak in the CV map, whereas we find a banana-shaped double peak; the minimum at O(2) on the C–O bond in Fig. 1(*a*) is about 0·3 e Å^{-3} deeper than that in the CV map; there is a deep minimum of −0·4 e Å^{-3} at N(1) inside the ring in Fig. 1(*a*) which is not present in the CV map (−0·1 e Å^{-3}); there is a minimum of more than −0·2 e Å^{-3} at H(2) in the CV map which is not present in our map. A second *X–N* map (Fig. 1*b*) was calculated with the scale factor determined from the molecular model of the density distribution described by Kutoglu & Hellner (1978), but with the same atomic (*i.e.* neutron) parameters. The scale (as factor of F_c) is now 1·0062; there are nearly no changes in the bond density distributions, but already noticeable changes in the difference density at the nuclear positions. At all nuclear positions [except for N(1)], a decrease of the difference density of 0·10–0·15 e Å^{-3} is induced by the increase in scale of 0·62%, a result in general agreement with the conclusions and results of Stevens & Coppens (1975).

The corresponding *X–X*(1*s*²) maps are presented in Fig. 2. In Fig. 2(*a*) the scale factor (1·0139) was obtained from refinement of the free-atom model, in Fig. 2(*b*) (1·0181) from refinement of the molecular density model. Again, the increase in scale of 0·42% (in Fig. 2*b*) induces a decrease of the difference density of 0·04–0·12 e Å^{-3} at the nuclear positions.

In the N–H and C–N bonds, and in the C–O bond peaks, the *X–N* and the *X–X*(1*s*²) maps differ only insignificantly (not more than one line, 0·1 e Å^{-3}). Larger discrepancies are observed around the O atoms. In the *X–X*(1*s*²) maps, the regions around O(1) and O(2) are more similar to each other [particularly in Fig. 2(*b*)] than in the *X–N* maps. These show a large polarization for O(2) but a small polarization for O(1). In the *X–N* maps, the polarization minima are more distant from the O nuclei (on the C–O bonds), whereas in the *X–X*(1*s*²) maps, they nearly coincide with the nuclear positions. Furthermore, in the *X–N* maps, there is a deep minimum (−0·4 e Å^{-3}), which is much weaker in the *X–X*(1*s*²) maps (−0·2 e Å^{-3}), at N(1) inside the ring. The peaks are generally a little lower in the *X–X*(1*s*²) maps.

Discussion

We shall discuss the following questions:

(1) How does the larger flatness of the lone-pair regions arise in the *X–X*(1*s*²) maps?

(2) Can the minima at the O atoms in the *X–X*(1*s*²) maps be interpreted as arising from polarization?

(3) Is the difference of polarization at O(1) and O(2), as observed in the *X–N* maps, likely to be valid?

The general flattening in the X–$X(1s^2)$ maps results from the larger thermal smearing of the C(1), C(2) and O(2) atoms in these maps. The larger thermal smearing causes the minima at the nuclear positions to decrease (because less density is now subtracted in the nuclear region) and simultaneously causes the adjacent bond peaks to decrease (because more density is now subtracted in the region more remote from the nuclei). The exception is given by the smaller $1s^2$ vibration tensor of O(1) which should give rise to an enhancement of the lone-pair regions at O(1). But this is not the case, perhaps because most of the lone-pair density is concentrated too close to the nucleus. In addition to the thermal smearing, the $1s^2$ location of O(2), being 0·004 Å closer to the lone-pair region, causes more density to be subtracted in the lone-pair region and less in the bond region close to O(2).

At first glance it appears that, in the X–$X(1s^2)$ maps, the minima at O(1) and O(2) are both due to polarization, particularly in Fig. 2(*b*). But this view can be ruled out by the fact that the minima are very close to the nuclear positions and only a little displaced towards the C atoms. The quantum-chemical calculation (Scheringer, Kutoglu, Hellner, Hase, Schulte & Schweig, 1978, referred to as SKHHSS) shows that, with polarization, the O nuclei are located approximately on the zero level of the difference density, and the minima clearly on the O—C bonds. Thus, it appears that the minima at the O atoms in the X–$X(1s^2)$ maps can be interpreted only to a small extent as polarization effects. With O(1), the effects of the vibration tensor and scale factor on the difference density do not (partially) compensate for each other, but rather add up so as to generate a deep minimum at the nucleus; with O(2), the minimum in Fig. 2(*b*) is caused only by the increase of the scale factor [in Fig. 2(*a*) the minimum is fairly weak, $-0{\cdot}1$ e Å^{-3}].

To discuss the differences of polarization at O(1) and O(2) in the X–N maps, we make use of the fact that, with O(2), the $1s^2$ position is displaced by 0·004 Å towards the lone-pair region, whereas, with O(1), the $1s^2$ position and the nuclear position practically coincide. [For O(2), the difference of the positions was classified as being significant by means of the statistical tests.] These facts suggest that there are different physical situations at O(1) and O(2); in particular it appears that O(2) is strongly polarized and O(1) only little or not at all. With the polarization of O(2) the negative charge is displaced so as to create the appearance of a longer bond, and the $1s^2$ positional parameters of O(2) are obviously adjusted in this sense. The large polarization of O(2) found in the X–N maps (Fig. 1) is in agreement with the theoretical difference density for the isolated molecule, and also with respect to the position of the minimum (SKHHSS, Fig. 2).

Although the difference of polarization at O(2) and O(1) is suggested by the facts, it is difficult to find a physical reason for it. Perhaps the deficiency of polarization at O(1) is due to the formation of a stronger hydrogen bond. The hydrogen bond O(1)···H(1)—N(1) is shorter (2·778 Å) and has a higher N—H stretching frequency (321·0 mm^{-1}) than the O(2)···H(2)—N(2) bond (2·798 Å, 306·0 mm^{-1}) (Verschoor & Keulen, 1971). Perhaps the deep minimum at N(1) inside the ring in the X–N maps is also due to the formation of the stronger hydrogen bond N(1)—H(1)···O(1); otherwise, no explanation can be given.

We think that a determination of the atomic parameters by means of a $1s^2$ core refinement can lead to significant errors with polarized atoms, particularly in the positional parameters. On the other hand, with unpolarized atoms, the $1s^2$ core refinement can well produce reliable results, as is confirmed by this investigation for the other atoms in cyanuric acid, and by the results obtained for hexamethylenetetramine (Stevens & Hope, 1975), and for deutero-oxalic acid dihydrate (Coppens, 1971). To what extent the nuclear parameters are falsified by the simple way of recalculating them for the temperature of the X-ray data, we cannot judge. The errors in the scale factors and atomic parameters primarily affect the density distribution around the nuclei and affect the bond densities much less. The differences between the X–N and X–$X(1s^2)$ maps show that, for cyanuric acid, we may have to accept uncertainties up to 0·4 e Å^{-3} at the nuclear positions, whereas we are better off with 0·15 e Å^{-3} in the bonding regions.

References

ABRAHAMS, S. C. & KEVE, E. T. (1971). *Acta Cryst.* A**27**, 157–165.

COPPENS, P. (1971). *Acta Cryst.* B**27**, 1931–1938.

COPPENS, P. & VOS, A. (1971). *Acta Cryst.* B**27**, 146–158.

HAMILTON, W. C. (1969). *Acta Cryst.* A**25**, 194–204.

International Tables for X-ray Crystallography (1974). Vol. IV. Birmingham: Kynoch Press.

KUTOGLU, A. & HELLNER, E. (1978). *Acta Cryst.* B**34**, 1617–1623.

SCHERINGER, C., KUTOGLU, A., HELLNER, E., HASE, H. L., SCHULTE, K. W. & SCHWEIG, A. (1978). *Acta Cryst.* B**34**, 2162–2165.

STEVENS, E. D. & COPPENS, P. (1975). *Acta Cryst.* A**31**, 612–619.

STEVENS, E. D. & HOPE, H. (1975). *Acta Cryst.* A**31**, 494–498.

VERSCHOOR, G. C. & KEULEN, E. (1971). *Acta Cryst.* B**27**, 134–145.